IJC
International Journal of Cancer

# GPER-induced signaling is essential for the survival of breast cancer stem cells

Yu-Tzu Chan[1]*, Alan C.-Y. Lai[2,3]*, Ruey-Jen Lin[1], Ya-Hui Wang[1], Yi-Ting Wang[4], Wen-Wei Chang[5], Hsin-Yi Wu[6], Yu-Ju Lin[1], Wen-Ying Chang[1], Jen-Chine Wu[1], Jyh-Cherng Yu[7], Yu-Ju Chen[4] and Alice L. Yu[1,8,9]

[1]Institute of Stem Cell and Translational Cancer Research, Chang Gung Memorial Hospital at Linkou and Chang Gung University, Taoyuan, Taiwan
[2]Institute of Biochemical Science, College of Life Science, National Taiwan University, Taipei, Taiwan
[3]Taiwan International Graduate Program, Academia Sinica, Taipei, Taiwan
[4]Institute of Chemistry, Academia Sinica, Taipei, Taiwan
[5]School of Biomedical Sciences and Department of Medical Research, Chung Shan Medical University, Taichung, Taiwan
[6]Instrumentation Center, National Taiwan University, Taipei, Taiwan
[7]Department of Surgery, Tri-Service General Hospital, Taipei, Taiwan
[8]Department of Pediatrics, University of California in San Diego, San Diego, CA
[9]Genomic Research Center, Academia Sinica, Taipei, Taiwan

**G protein-coupled estrogen receptor-1 (GPER), a member of the G protein-coupled receptor (GPCR) superfamily, mediates estrogen-induced proliferation of normal and malignant breast epithelial cells. However, its role in breast cancer stem cells (BCSCs) remains unclear. Here we showed greater expression of GPER in BCSCs than non-BCSCs of three patient-derived xenografts of $ER^-/PR^+$ breast cancers. GPER silencing reduced stemness features of BCSCs as reflected by reduced mammosphere forming capacity *in vitro*, and tumor growth *in vivo* with decreased BCSC populations. Comparative phosphoproteomics revealed greater GPER-mediated PKA/BAD signaling in BCSCs. Activation of GPER by its ligands, including tamoxifen (TMX), induced phosphorylation of PKA and BAD-Ser118 to sustain BCSC characteristics. Transfection with a dominant-negative mutant BAD (Ser118Ala) led to reduced cell survival. Taken together, GPER and its downstream signaling play a key role in maintaining the stemness of BCSCs, suggesting that GPER is a potential therapeutic target for eradicating BCSCs.**



*Y.-T.C. and A.C.-Y.L. contributed equally to this work

**Author contributions:** Conception and design: Chen Y-J, Yu AL, Lai AC-Y, Chan Y-T, Chang W-W. Performed research: Lai AC-Y, Chan Y-T, Wang Y-T, Wu H-Y, Lin R-J, Lin Y-J, Wang Y-H, Chang W-Y, Wu J-C. Provision of clinical specimens: Yu J-C. Manuscript writing: Lai AC-Y, Chan Y-T, Yu AL. Final approval of manuscript: Chen Y-J, Yu AL. Review of the manuscript: all authors.

**Additional Supporting Information** may be found in the online version of this article.

**Key words:** GPER, breast cancer stem cell, phosphoproteomics, BAD, tamoxifen

**Abbreviations:** 4-OHT: 4-hydroxytamoxifen; ALDH: aldehyde dehydrogenases; BCSC: breast cancer stem cell; CTTN: cortactin; DEAB: diethylaminobenzaldehyde; E2: 17β-estradiol; E3: estriol; EGFR: epidermal growth factor receptor; ER: estrogen receptor; GPCR: G protein-coupled receptor; GPER: G protein-coupled estrogen receptor-1; HER2: human epidermal growth factor receptor 2; IMAC: immobilized metal affinity chromatography; LC–MS/MS: liquid chromatography-tandem mass spectrometry; MAPK: mitogen-activated protein kinase; PDX: patient-derived xenograft; PR: progesterone receptor; RFS: relapse-free survival; SERM: selective estrogen receptor modulator; shRNA: short hairpin RNA; TMX: tamoxifen; WT: wild-type

**Conflict of interest:** Authors declare no conflict of interests.

**Grant sponsor:** Academia Sinica; **Grant number:** 97-2628-M-001-020-MY3; **Grant sponsor:** Chang Gung Medical Foundation; **Grant numbers:** OMRPG3C0012, OMRPG3C0013; **Grant sponsor:** Ministry of Science and Technology in Taiwan; **Grant numbers:** MOST 103-2321-B-182A-002, MOST 104-2321-B-182A-004, NSC102-2321-B-182A-005



**DOI:** 10.1002/ijc.32588

**History:** Received 24 Oct 2018; Accepted 25 Jun 2019; Online 24 Jul 2019

**Correspondence to:** Yu-Ju Chen, Institute of Chemistry, Academia Sinica, Taipei, Taiwan, Tel.: +886-2-27898660, Fax: +886-2-27831237, E-mail: yujuchen@gate.sinica.edu.tw; or Alice L. Yu, Institute of Stem Cell and Translational Cancer Research, Chang Gung Memorial Hospital at Linkou and Chang Gung University, Taoyuan, Taiwan, Tel.: +886-3-3281200, Fax: +886-3-3285060, E-mail: a1yu@ucsd.edu

**What's new?**

**G protein-coupled estrogen receptor-1 (GPER) mediates estrogen-induced proliferation of normal and malignant breast epithelial cells. However, the role of GPER in breast cancer stem cells (BCSC) biology remains unclear. Here, using patient-derived xenografts of ER−/PR+ breast cancer, the authors found higher expression of GPER in BCSCs than non-BCSCs. Moreover, the results indicated that stemness features were sustained *via* GPER-mediated PKA/BAD phosphorylation. Stimulation by the GPER ligand tamoxifen enhanced BCSC cell viability and population and BAD phosphorylation. The findings revealed a vital role of GPER-mediated signaling pathways in BCSC survival, suggesting GPER as a potential therapeutic target for eradicating BCSCs.**

## Introduction

The biological characteristics and clinical behavior of breast cancer are heterogeneous; breast cancer subtypes are assigned according to the presence of three receptors: the estrogen receptor (ER), the progesterone receptor (PR) and human epidermal growth factor receptor 2 (HER2). Estrogens, as ligands of the ER, control the normal growth and differentiation of human breast epithelial cells, and long term exposure to an excess amount of estrogen may promote the development of breast cancer.[1] Approximately 70% of breast cancers express hormone receptors and are amenable to endocrine therapy. Tamoxifen (TMX), the most commonly used antiestrogen drug, is a selective ER modulator (SERM) that activates/inhibits ER in cell type- and context-dependent manner.[2] Another antiestrogen drug, fulvestrant, destabilizes ER upon binding and promotes ER degradation.[3] Besides these SERMs, aromatase inhibitors are effective as therapeutic agents by blocking estrogen production.[4] However, about one-third of patients treated with adjuvant TMX develop aggressive recurrent disease, which is attributed to the activation of escape pathways, providing tumors with alternative proliferative and survival stimuli.[5] Emerging evidence has implicated G protein-coupled estrogen receptor-1 (GPER, formerly known as GPR30) in TMX resistance. Binding of estrogen to GPER, a member of the G protein-coupled receptor (GPCR) superfamily, activates adenylyl cyclase, causing the release of cAMP.[6] In addition, estrogen activates GPER to promote epidermal growth factor receptor (EGFR) dimerization and downstream activation of the mitogen-activated protein kinase (MAPK) signaling axis.[7] It has been reported that GPER activation stimulates the migration of breast cancer cells *in vitro*, and promotes metastasis *in vivo*.[8,9] Of note, ER antagonists such as TMX and fulvestrant act as agonists for GPER and stimulate cell proliferation.[10,11] Moreover, binding of TMX to GPER induced aromatase expression to sustain TMX-resistant breast cancer cell growth.[12] These findings are in line with the clinical observation that TMX treatment resulted in poorer relapse-free survival (RFS) in patients with GPER-positive tumors than those with GPER-negative tumors.[13] In contrast to the above-mentioned tumorigenic role of GPER, a few studies have shown that GPER can act as an inhibitor on the proliferation of breast cancer cells.[14] Besides, the role of GPER in breast cancer stem cells (BCSCs) has yet to be addressed.

The existence of cancer stem cells, which exhibit the stem cell-like properties of self-renewal and differentiation, has been well-documented.[15] In breast cancer, cells with a $CD44^{+}CD24^{-/low}$ surface antigen profile or those with high activities of aldehyde dehydrogenases (ALDH) are considered to be enriched BCSCs, based on their capacity for mammosphere formation *in vitro* and tumorigenesis *in vivo* and their ability for yielding heterogeneous phenotypes including non-$CD44^{+}CD24^{-/low}$ or $ALDH^{low}$ population.[16] Approximately 74% of recurrent tumors contain a subpopulation of $CD44^{+}CD24^{-/low}$ cells as compared to 9% of tumors in untreated patients, implying that BCSCs may be more resistant to therapy and, therefore, an important target for treating breast cancer.[15] Indeed, BCSCs are relatively resistant to radiation and chemotherapy, accounting for their increased frequency in residual tumor after fractionated irradiation[17] or chemotherapy.[18] Finally, an increased percentage of $CD44^{+}CD24^{-/low}$ or $ALDH^{high}$ cells has also been observed in tumors that remain after neoadjuvant endocrine therapy, suggesting a subpopulation of hormone-resistant BCSCs.[18,19] Consistent with the unique properties that confer BCSC resistance to therapy, BCSCs have been reported to undergo constitutive activation of signal transduction pathways related to stem-cell functions. It has been shown that the PTEN/mTOR/STAT3 pathway is essential in maintaining the survival and proliferation of the cancer stem cell-like subpopulation of the MCF-7 breast cancer cell line.[20] Likewise, the IGF-1R/PI3K/AKT/mTOR pathway has been reported to regulate BCSC proliferation.[21] Although the aforementioned signal transduction pathways appear to affect BCSC biology, most of these studies used cancer cell lines that have been passaged *in vitro* for years and may not reflect the true biology of BCSCs *in vivo*. A thorough understanding of the nature of BCSCs requires a systematic and in-depth analysis of the signal transduction abnormalities within BCSCs harvested from patient-derived xenografts (PDXs), which may enhance the knowledge on cancer pathogenesis and unveil novel therapeutic targets.

To elucidate the roles of GPER in BCSCs, we applied a quantitative phosphoproteomics analysis to systematically compare the BCSCs and non-BCSCs isolated from a PDX of $ER^{-}$ breast cancer to better understand the roles of GPER in BCSCs and to elucidate GPER-mediated signaling contributing to BCSC biological features. We uncovered a complex interplay of upregulated signaling pathways associated with the stemness and survival of BCSCs. Among the differentially regulated pathways, we showed that PKA/BAD is one of signaling cascades regulated by GPER in BCSCs, which offers an alternative mechanism of estrogen-mediated BCSC survival, in addition to the well-known ER pathway.

## Materials and Methods

### Isolation and maintenance of primary human breast cancer xenografts

Isolation of primary tumor cells and maintenance of xenografts were performed as previously described.[22] Briefly, the tumor specimens were enzymatically digested by collagenase (1,000 U/ml), hyaluronidase (300 U/ml), and DNase I (100 μg/ml) at 37°C for 1 hr. Then, tumor cells were filtrated through a 100 μM cell strainer and removed from red blood cells and dead cells by Percoll density gradient centrifugation. Cells resided in buffy coat were washed and resuspended by RPMI1640 medium supplemented with 5% FBS for flow cytometric analysis.

### Cell culture and reagents

AS-B145 and AS-B634 cells were derived from $H2K^{d-}CD24^{-}CD44^{+}$ BCSCs of the BC0145 and $H2K^{d-}ALDH^{+}$ BCSCs of the BC0634 xenograft, respectively, and cultured in modified Eagle's medium, 10% (v/v) fetal bovine serum, 10 μg/ml insulin at 37°C with 5% $CO_2$.[22,23] E2 (Cat. #10006315), E3 (Cat. #10006484) and G1 (Cat. #100088933) were purchased from Cayman Chemical (Ann Arbor, MI). 4-Hydroxytamoxifen (4-OHT; Cat. #H7904) was purchased from Sigma (St. Louis, MO).

### RT-qPCR of GPER mRNA

Total RNA from AS-B145 cells was isolated using TRIzol reagent (Cat. #15596–026, Invitrogen, Carlsbad, CA). Total RNA (1 μg) was reverse transcribed into cDNA using TaqMan Reverse Transcription Reagents (Cat. #N8080234, Applied Biosystems, Foster City, CA). FastStart SYBR Green Master (Cat. #04673484001, Roche Applied Science, Indianapolis, IN) was used for RT-qPCR and analyzed using a 7300 Sequence Detection System (Applied Biosystems). Briefly, 10 ng of cDNA and GPER-specific primers were used for qPCR amplification. The threshold cycle (Ct) values were determined using the default threshold settings. Total initial RNA was normalized to the Ct values of the internal control, GAPDH. The primer sequences for GPER, GPERF01 and GPERR01, are shown in Supporting Information Table S2.

### Knockdown of GPER expression by lentiviral short hairpin RNA

All lentiviral short hairpin RNA (shRNA) plasmids are listed in Supporting Information Table S3. These shRNAs were purchased from the National RNAi Core Facility of the Institute of Molecular Biology/Genomics Research Center, Academia Sinica, Taiwan. The shRNA plasmid against luciferase served as a negative control (shLuc). The procedure for lentiviruses production was described previously.[22] At 24 hr after seeding, cells were infected by viruses at a multiplicity of infection (MOI) of 2 with the addition of 8 μg/ml polybrene (Sigma-Aldrich, St. Louis, MO). Puromycin (Sigma-Aldrich) selection (2 μg/ml) was administered 24 hr after infection.

### Gel-assisted digestion and IMAC-facilitated phosphopeptide purification

Cells were lysed in 0.25 M Tris–HCl (pH 6.8) and 1% (w/v) SDS. Cell lysate protein samples (800 μg) spiked with 0.1 μg of β-casein (internal standard) were each incorporated directly into an acrylamide gel (acrylamide/bisacrylamide solution (40%, (v/v), 29:1), 10% (w/v) ammonium persulfate, 100% *N*,*N*,*N*′,*N*′-tetramethylenediamine at a 14.5:0.7:0.3 ratio) in an Eppendorf tube. Each gel was chopped into pieces and washed three times with 50% (v/v) acetonitrile (ACN) in 25 mM triethylammonium bicarbonate (TEABC) to remove detergent. The gels were then dehydrated by soaking in 100% ACN and were completely dried by vacuum centrifugation in a Savant SpeedVac® concentrator (Thermo Fisher Scientific, Waltham, MA). For proteolysis, each dried gel sample was immersed in 25 mM TEABC that contained trypsin (protein/trypsin = 40:1, w/w) and was incubated overnight at 37°C. Tryptic peptides were extracted three times in 5% (v/v) formic acid (FA)/50% (v/v) acetonitrile (ACN) for 30 min and completely dried by vacuum centrifugation at room temperature. IMAC was performed as previously described with minor modifications.[24,25] The IMAC column was enclosed in a stainless steel column that was fitted with a 0.5-μm frit disk at one end. Ni-NTA resin (Qiagen, Germantown, MD) was packed in a 10-cm microcolumn (500-μm i.d. PEEK column, Upchurch Scientific/Rheodyne, Oak Harbor, WA) for phosphopeptide purification, which was performed using an autosampler, an HP1100 solvent delivery system (Hewlett-Packard, San Jose, CA) with a flow rate of 13 μl/min, and a loading/conditioning buffer of 6% (v/v) acetic acid (pH 3.0). The enrichment protocol consisted of the following steps: (*i*) removal of $Ni^{2+}$ with the addition of 100 μl of 50 mM EDTA in 1 M NaCl; (*ii*) activation of the IMAC column with 100 μl of 0.2 M $FeCl_3$ and equilibration with loading buffer for 30 min; (*iii*) loading of peptide samples in loading buffer onto the IMAC column; (*iv*) removal of unbound peptides with 100 μl of 25% (v/v) ACN, followed by equilibration with loading buffer for 15 min; (*v*) elution of bound peptides in 100 μl of 200 mM $NH_4H_2PO_4$ and drying by vacuum centrifugation prior to desalting and concentration using ZipTips (Millipore, Burlington, MA).

### Liquid chromatography-tandem mass spectrometry

Purified phosphopeptides were dissolved in aqueous 0.1% (v/v) TFA. For LC–MS/MS (Q-TOF Premier mass spectrometer, Waters Corp., Milford, MA), samples were individually injected into a 2-cm × 180-μm capillary-trap column and separated through a 75-μm × 25-cm nanoACQUITY 1.7-μm BEH C18 column controlled by a nanoACQUITY Ultra-Performance LC system (Waters Corp). Peptides were eluted in aqueous 0.1% FA that contained a gradient of 0–80% ACN over 120 min. The mass spectrophotometer was operated in the ESI-positive V mode with a resolving power of 10,000. A NanoLockSpray source was used for accurate mass measurement, and the lock mass channel was sampled every 30 s. The

spectrometer was calibrated with a synthetic human [Glu[1]]-fibrinopeptide B (1 pmol/μl, Sigma Aldrich) delivered through the NanoLockSpray source. Data acquisition was operated in the data-directed mode and included a full MS scan (400–1,600 *m*/*z*, 0.6 s) and three MS/MS scans (100–1,990 *m*/*z*, 1.2 s per scan) of the three most intense ions in the full scan mass spectrum.

### Database searching and quantification by IDEAL-Q

Quantification of proteins in the phosphoproteome was performed as previously described with minor modifications.[25,26] Raw MS/MS data were converted into peak lists using Distiller (Matrix Science, Boston, MA; version 2.0) and default parameters. All MS/MS samples were subjected to a Mascot (Matrix Science; version 2.2.1) search of the IPI_HUMAN_3.29 (version 3.29, 68,161 entries) and Swiss-Prot_Metazoa_Animals (version 54.2, 17,170 entries) databases with the following parameters. The parent- and fragment-ion mass tolerances were each 0.1 Da. Two missing tryptic cleavages were allowed. Ser/Thr/Tyr phosphorylation and Met oxidation were allowed but not required. The protein identification was based on the significant Mascot score ($p < 0.05$). The raw data were converted into mzXML-formatted files, and the MASCOT search results were exported into eXtensive Markup Language data (.XML)-formatted files. Quantification of the extracted ion chromatogram (XIC) of each phosphopeptides and the fold-change were performed using IDEAL-Q.[26]

### Bioinformatics

For the annotation of subcellular localization, molecular function and biological process, the proteins were characterized by GoMiner.[27] To identify signaling pathways that contained the differentially regulated phosphoproteins, the pathway analysis tool MetaCore was used and augmented by literature mining.[28] The resulting annotation was organized using Excel and presented in graphical formats.

### Tumorigenicity *in vivo*

AS-B145 and AS-B634 cells were infected with lentiviral shRNAs for 6 days. shGPER clone #B was used for GPER knockdown. A total of $1 \times 10^5$ or $5 \times 10^4$ of the viable puromycin-resistant AS-B145 or AS-B634 cells were mixed with matrigel for subcutaneous injection into the mammary fat pads of 6 or 5 NSG mice, respectively. Tumor formation was monitored weekly after inoculation.

### Statistical analysis

The significance of the cell proliferation experiments was determined by one-way ANOVA with Holm-Sidak's multiple comparisons. To compare the growth of AS-B145 cells expressing the mutant BAD (Ser118Ala), wild-type BAD and vector, cell index at 96 hr was analyzed. The effects of chemicals treatment on $GPER^+$ population and $ALDH^+$ population were analyzed by one-way ANOVA with Holm–Sidak's multiple comparisons. For mammosphere formation and mean percentages of $ALDH^+$ cells in the total tumor cell population experiments, data were presented as mean ± SD and analyzed by Student's *t*-test. A value of $p < 0.05$ was considered as significant.

### Data availability

Data available on request from the authors.

## Results

### Greater expression of GPER in BCSCs than in non-BCSCs

To examine the role of GPER in BCSCs, we exploited our previously established PDXs of breast cancer, including BC0145, BC0244 and BC0634, in which their BCSCs were identified as $H2K^{d-}CD24^-CD44^+$ subpopulation for BC0145 and BC0244 and $H2K^{d-}ALDH^+$ for BC0634, based on their higher tumorigenicity and re-emergence of tumor heterogeneity as the parental tumors.[21,23] The clinical–pathological features of these three tumors are shown in Figure 1*a*. Both BC0145 and BC0634 tumor were ER-negative, PR-positive and HER2-positive. BC0244 was ER-negative, PR-positive and HER2-negative. The expression of GPER in the BCSCs and non-BCSCs of the three PDXs was examined by western blotting. As shown in Figure 1*b*, multiple bands of GPER were detected in the BCSCs of each of the three tumors, which might reflect posttranslational modifications in the form of *N*-linked glycosylation or ubiquitination.[29,30] GPER silencing by shRNA revealed that multiple bands with a molecular mass of 50–55 kDa were GPER (Fig. 2*a*). When normalized to the GAPDH band of the corresponding samples, the amounts of GPER in BCSCs from all three PDXs were higher than their non-BCSC counterparts (Fig. 1*b*). To further validate the greater abundance of GPER-positive cells in the BCSC population, we first identified CSC-enriched and non-CSC populations of cancer cells derived from PDXs BC0145 and BC0244, based on their CD44/CD24 phenotypes (Fig. 1*c*), and determined their expression of GPER by FACS analyses. For BC0145, 29.7% of the cells were $GPER^+/CD44^+$ and 10.2% were $GPER^+/CD44^-$. For BC0244, 44.8% of the cells were $GPER^+/CD44^+$ and only 4.7% were $GPER^+/CD44^-$. The results showed that $GPER^+$ cells were enriched in the CSC population, suggesting that GPER may play a role in the maintenance of BCSC properties.

### Knockdown of GPER reduced the viability and stemness of BCSCs

To decipher the importance of GPER in maintaining BCSC characteristics, we knocked down GPER expression with specific shRNAs (shGPERs) in AS-B145, a cell line derived from BCSCs of BC0145.[21] After infection of AS-B145 cells with three shGPER clones, GPER expression was decreased to 43 and 56% of control by clone B and C, respectively (Fig. 2*a*, left panel). The proliferation of shRNAs infected AS-B145 cells was monitored using the xCELLigence system. As shown in Figure 2*a* (center panel), shGPER infected cells had a lower

(a)

| Coding | Clinical stage | Histology (Grade) | ER | PR | HER2 |
|---|---|---|---|---|---|
| BC0145 | IIIC | Infiltrating ductal carcinoma (IDC) (III) | — | + (80%) | + |
| BC0244 | IIIB | Residual sarcoma post neoadjuvant therapy; Carcinosacroma (III) | — | + (70%) | — |
| BC0634 | IIIA | IDC (III) | — | + (30%) | + |

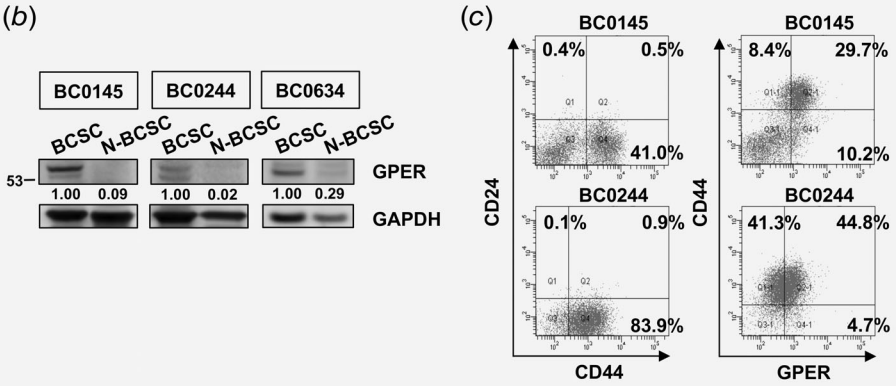


**Figure 1.** Greater expression of GPER in BCSCs than in non-BCSCs. (*a*) Clinical characteristics of the three patients with breast cancer BC0145, BC0244 and BC0634, from whom the xenografts were derived. (*b*) Total cell lysates from BCSCs and non-BCSCs sorted from xenografts of BC0145, BC0244 and BC0634 were subjected to western blotting. GPERs were detected at the bands with a molecular weight in the 50–55 kDa region. GAPDH protein served as the internal control for normalization. For normalization, total GPER expressions in BCSCs of BC0145, BC0244 and BC0634 were each set as 1.0 for comparison to values in non-BCSCs. N-BCSC: non-BCSC. (*c*) Tumor cells from BC0145 and BC0244 xenografts were analyzed for the expression of surface antigens CD24, CD44 and total GPER by flow cytometry. After cells staining for CD24/CD44, cells were fixed and permeabilized for GPER staining.

cell index than controls, indicating that GPER depletion impeded cell growth. To further confirm this, we also silenced GPER expression in another ER-negative BCSC cell line, AS-B634, which was derived from BCSCs of the BC0634 PDX. Effective silencing of GPER expression to 9, 5 and 20% of control by shRNA clones A, B and C, respectively, was observed in AS-B634 cells (Fig. 2*a*, left panel) along with significant suppression of the proliferation of shGPER infected cells (Fig. 2*a*, right panel). We also verified the role of GPER in BCSC ($H2K^{d-}/CD24^{-}/CD44^{+}$ cells) freshly isolated from the BC0145 xenograft. As shown in Figure 2*b*, mRNA and protein level of GPER declined to 50 and 62% of control by shGPER clone B (sh-B), respectively. Similar results were observed in $H2kd^{-}$ BC0634 cells, which were freshly isolated from BC0634 xenograft. The GPER expression of mRNA and protein were silenced to 24 and 45% of control by clone B in BC0634. Furthermore, the proliferation of shRNAs infected BC0145 and BC0634 cells was significantly stunted in shGPER infected cells as shown in Figure 2*c*. Next, we examined the effect of GPER silencing on their mammosphere-forming capacity. As shown in Figure 2*d*, the average numbers of mammospheres formed diminished from $18.2 \pm 1.3$ to $7.5 \pm 1.4$ for BC0145 cells infected with control shRNA (shLuc) and shGPER, respectively ($p < 0.001$). Similar results were observed in BC0634, with the reduction in the number of mammospheres from $8.2 \pm 2.1$ to $1.7 \pm 1.3$ ($p < 0.001$) for cells infected with shLuc and shGPER, respectively.

## Identification of the key cellular machinery in BCSCs revealed by phosphoproteomics

To decipher the GPER-related signaling pathway contributing to BCSC properties, we applied quantitative phosphoproteomic analysis to systematically compare the CSCs and non-CSCs of BC0145 using our previously reported informatics-assisted label-free mass spectrometry approach.[25,26] After the internal standard β-casein was added to the cell lysate of isolated CSCs and non-CSCs in equal amounts, after which the samples were subjected to gel-assisted trypsin digestion. The phosphopeptides were subsequently purified by immobilized metal affinity chromatography (IMAC)[24] and then subjected to liquid chromatography-tandem mass spectrometry (LC–MS/MS) in triplicate (Fig. 3*a*). Quantitative analysis of all identified phosphopeptides was performed using IDEAL-Q. A total of 835 phosphopeptides from 455 proteins were confidently identified (false-discovery rate < 1%) from two separate replicates. Detailed information on their identification and relative quantitation between the BCSC and non-BCSC subpopulations are listed in Supporting Information Table S1. Phosphoproteins with at least twofold upregulation in BCSCs were analyzed by MetaCore to identify the key signaling pathways associated with BCSC characteristics. Top ranking pathways with

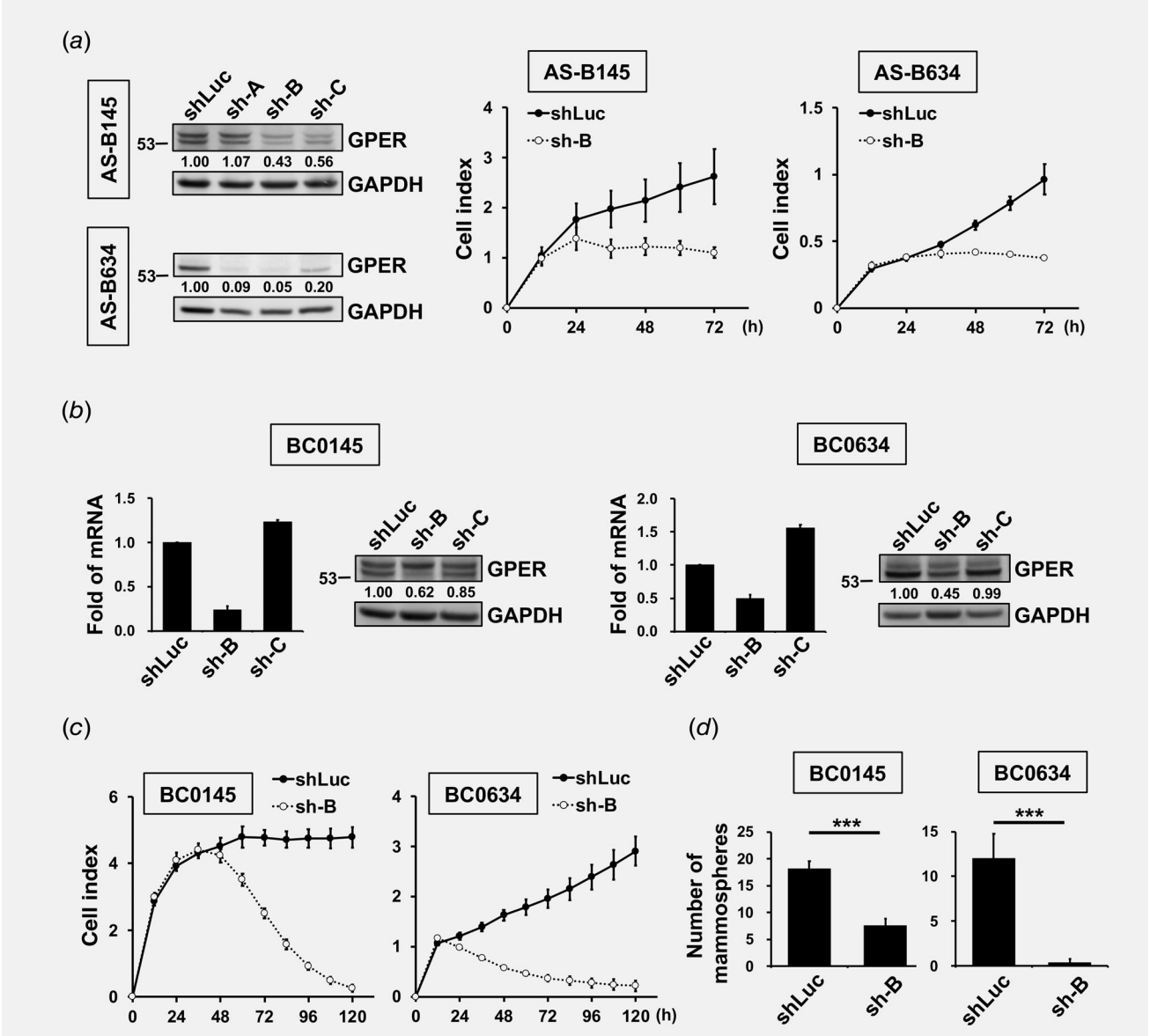


**Figure 2.** GPER regulation of the survival and stemness of BCSCs. (*a*) Left panel: AS-B145 or AS-B634 cells were infected with lentiviral shRNAs and the total proteins were harvested 6 days after infection for western blotting. GAPDH protein served as the internal control for normalization. The normalized total GPER expression of shLuc cells was set as 1.0 for comparison to values of shGPER infected cells (sh-A, sh-B and sh-C). Center and Right panels: the growth curve of shRNA infected AS-B145 (shLuc and sh-B) and AS-B634 (shLuc and sh-B) cells was determined using the xCELLigence system over a period of 72 hr. (*b*) $H2K^{d-}/CD24^{-}/CD44^{+}$ BC0145 cells (left panel) and $H2K^{d-}$BC0634 cells (right panel) were infected with shLuc, sh-B or sh-C. GPER mRNA and protein levels were determined by real-time qPCR and western blotting at 6 days after infection, respectively. The expression of GPER was presented as fold expression relative to shLuc. (*c*) The cell proliferation of shRNAs infected $H2K^{d-}/CD24^{-}/CD44^{+}$ BC0145 or $H2K^{d-}$ BC0634 cells were monitored by xCelligence system over a period of 120 hr. (*d*) Mammosphere formation was assessed for freshly sorted BCSCs from the BC0145 (left) and BC0634 xenograft (right) (2,000 cells/well in a 96-well plate format). Both cell types were infected with shLuc control or shGPER-B. ***$p < 0.001$ as compared to the control group using the Student's *t*-test.

most dramatic upregulation in BCSCs compared to non-BCSCs were those involved in cytoskeleton remodeling, translation initiation, cell survival and cell cycle progression, based on the corresponding GeneGo pathway maps (Fig. 3*b*) and GeneGo process networks (Fig. 3*c*). These processes may contribute to the known metastasis and differentiation characteristics in BCSCs.[15] All differentially expressed phosphoproteins were further annotated with molecular-function categories in GeneGo (Fig. 3*d*). The analysis revealed that elevated phosphoproteins were enriched in categories involved in the replication of cells (nucleotide-binding, RNA binding and transcription activity) and signal transduction (ATP binding, kinase activity, phosphatase activity, protein binding and receptor). However, the molecular functions of ~21% of these differentially regulated

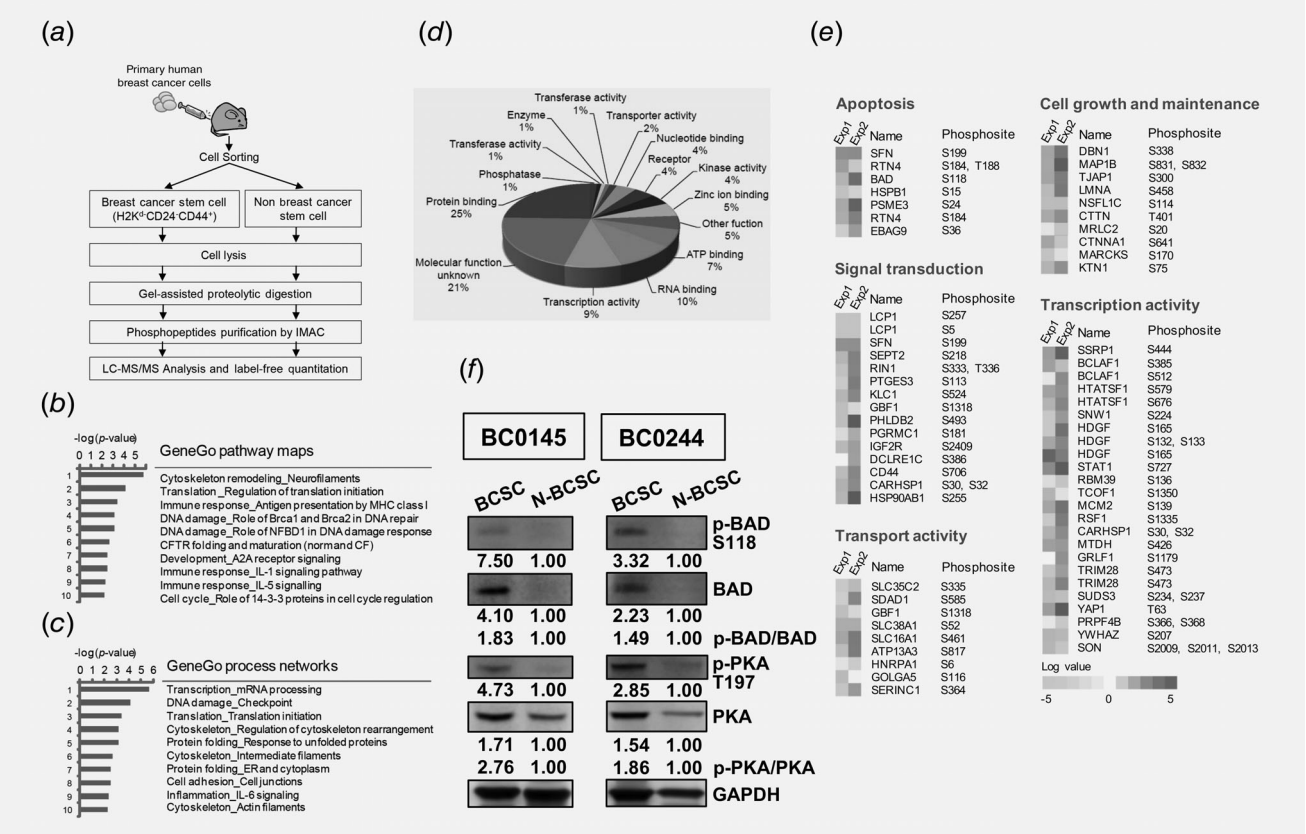


**Figure 3.** Functional analysis of differentially expressed phosphoproteins in BCSCs and non-BCSCs. (*a*) Workflow diagram for the phosphoproteomic study, which quantitatively compared the phosphoproteomes of the BCSCs and non-BCSCs sorted from the BC0145 xenograft. Equal amounts of BCSC and non-BCSC lysates, each containing the internal standard β-casein, were enzymatically digested, enriched in phosphopeptides by IMAC and subjected to triplicate LC–MS/MS. Quantification of the phosphopeptides was performed using IDEAL-Q software. The phosphoproteins having at least twofold greater expression in BCSCs than in non-BCSCs from two independent experiments performed in triplicate are shown. (*b*) The top 10 GeneGo pathway maps ($p < 0.001$). (*c*) The top 10 GeneGo process networks (*d*) GoMiner analysis showing the distribution of the classified molecular functions of differentially expressed phosphoproteins. (*e*) Heat maps for the differentially expressed phosphoproteins identified in duplicated experiments. Quantitative comparison revealed that most of the differentially expressed phosphoproteins are involved in cell adhesion, cell migration, secretion, cell motility or the cell cycle. (*f*) Validation of selected phosphoproteins. Phosphorylation states of selected phosphoproteins in BCSCs and non-BCSCs from BC0145 and BC0244 xenografts. Western blot analysis of total cell lysates from BC0145 and BC0244 BCSCs and non-BCSCs was performed with antibodies against BAD, BAD pSer118, PRKACA and PRKACA pThr197. The ratios of expression levels were calculated for the BCSC and non-BCSC proteins after normalization of their respective signals to the corresponding GAPDH signal. The blots of GAPDH were identical to those in Figure 1*b* since the western blot were derived from the same experiment.

phosphoproteins are unknown, making them interesting candidates for future pursuits of their roles in BCSC. Figure 3*e* showed the heat map of differentially expressed phosphoproteins in two independent experiments, grouped into five functional categories in relation to tumorigenesis (apoptosis, signal transduction, transporter activity) and *stem cell* characteristics (cell growth and maintenance, transcription activity). The elevated phosphorylation levels of almost all of these proteins implicated their roles in BCSC growth and maintenance, which are supported by published studies, including the following examples. (*i*) For apoptosis, BAD p-Ser118 was 6.5-fold greater in BCSCs than in non-BCSCs, which is consistent with observations that BAD p-Ser118 can prevent apoptosis in cancer cells and the expression of BAD can be used as a marker for chemoresistance of breast cancer.[31] (*ii*) For cell growth and maintenance, we found that phosphorylation of Cortactin (CTTN), which is a key player in tumor cell migration,[32] was increased up to 4.5-fold in the BCSCs. (*iii*) For signal transduction, we found a 14.6-fold increase in phosphorylation of Ser706 in CD44 from the BCSCs (Supporting Information Table S1). The presence of phosphorylated CD44 p-Ser706 is required for hyaluronan-dependent, CD44-mediated growth of melanoma and prostate cancer.[33] (*iv*) For transcription activity, YAP1, a transcription cofactor, was reported to regulate stem cell self-renewal and differentiation.[34] We found that p-Thr63 of YAP1 was higher in BCSC than non-BCSC (Supporting Information Table S1). Further validation of greater expression of total YAP1 in BCSC was demonstrated in the PDXs (BC0145 and BC0244; Supporting Information Fig. S1). Another protein, STAT1, which requires phosphorylation at Ser727 for maximal transcriptional activity,[35] was found to have increased phosphorylation at p-Ser727 in BCSC *via*

phosphoproteomic analysis (Supporting Information Table S1). Indeed, western blot analysis of BC0145 confirmed that the level of STAT1 p-Ser727 in BCSC was 23.8-fold that of non-BCSCs, while the expression level of total STAT1 was upregulated by only 2.83-fold (Supporting Information Fig. S1).

### GPER-related signals were highly expressed in BCSCs

Phosphoproteomic analysis revealed that some GPER-related proteins or other proteins essential for CSCs properties, such as PKA and BAD, were more highly phosphorylated in BCSCs than in non-BCSCs (Supporting Information Table S1). It has been reported that PKA is an effector of GPCR signaling.[36] We speculated that GPER may act as an alternative ER by activating PKA signaling to promote $ER^-$ breast cancer progression. The PKA holoenzyme contains two cAMP-dependent protein kinase type I-alpha regulatory subunit (PRKAR1A)-like regulatory subunits and two cAMP-dependent protein kinase catalytic subunit alpha (PRKACA)-like catalytic subunits.[37] Hence, western blots using antibodies against PRKACA and phosphorylated PRKACA (PRKACA pT197) were performed to determine the activation status of PKA. As shown in Figure 3*f*, the relative expressions of PRKACA p-Thr197 and total PRKACA protein in BCSC samples of BC0145 were 4.73- and 1.71-fold, respectively, of those in non-BCSCs, after normalization to their corresponding GAPDH. When normalized to total PRKACA protein, the amount of PRKACA p-Thr197 in BCSCs was 2.76-fold of non-BCSCs. It has been reported that BAD, a downstream target of PKA, was highly expressed in CSCs and phosphorylation of BAD (Ser112 and Ser136) was essential for the survival of CSCs.[38] Our phosphoproteomes of BC0145 revealed another phosphorylation site of BAD at Ser118, which was more highly phosphorylated in BCSCs than in non-BCSCs (Supporting Information Table S1). Phosphorylation of Ser118 leads to the release of Bcl-$X_L$, thereby promoting cell survival.[39] As shown in Figure 3*f*, the relative expressions of p-BAD Ser118 and total BAD protein in BCSC samples of BC0145 were 7.50- and 4.10-fold, respectively, of those in non-BCSCs, after normalization to their corresponding GAPDH. When normalized to total BAD protein, the amount of p-BAD Ser118 in BCSCs was 1.83-fold of non-BCSCs. A similar trend was noted in another PDX, BC0244. After normalization to their corresponding total proteins, the relative abundance of PRKACA p-Thr197 and p-BAD Ser118 in BCSCs of BC0244 were 1.86- and 1.49-fold, respectively, of non-BCSC subpopulation (Fig. 3*f*).

### GPER-mediated BAD phosphorylation is essential for the maintenance of BCSC characteristics

To verify the role of BAD p-Ser118 in BCSCs, we incorporated the mutant BAD Ser118Ala gene into a doxycycline-inducible lentiviral vector and infected AS-B145 cells with the vector to create a stable clone (Supporting Information Materials and Methods). Cell proliferation was determined using the xCELLigence system. Doxycycline-induced expression of the dominant-negative BAD Ser118Ala mutant significantly suppressed the proliferation of AS-B145 cells, as compared to cells expressing wild-type (WT) BAD ($p < 0.001$; Fig. 4*a*). Based on these results, we hypothesized that GPER might trigger PKA-mediated signaling, causing the release of cAMP and induction of BAD Ser118 phosphorylation to maintain BCSCs properties. Since estrogens and the TMX metabolite 4-OHT can induce GPER-mediated signal transduction that promotes proliferation and survival in breast cancer cell lines,[36] we examined the possible induction of BAD Ser118 phosphorylation by these agonists of GPER. Incubation of AS-B145 cells with a pharmacological concentration of 4-OHT (2,500 nM) caused a time-dependent increase in the phosphorylation of BAD Ser118 over the 15–60 min time period (Fig. 4*b*). Upon 4-OHT treatment, phosphorylation of BAD at Ser118 increased to 1.63- to 1.80-fold of untreated cells. As expected, phosphorylation of another two serine residues of BAD (Ser112 and Ser136) known to be essential for the survival of CSCs also increased (Fig. 4*b*). Since treatment of AS-B145 cells with 4-OHT upregulated the phosphorylation of BAD Ser118, we anticipated that GPER ligands such as 4-OHT, 17β-estradiol (E2) and estriol (E3) might influence the survival of breast cancer cells. Indeed, incubation of AS-B145 and AS-B634 cells with any one of the three ligands for 72 or 48 hr increased the growth of both types of cell, respectively (Figs. 4*c* and 4*d*). In addition, the effect of GPER activation on promoting cell growth was further confirmed by treatment of AS-B145 and AS-B634 cells with G1, a specific GPER agonist (Figs. 4*c* and 4*d*). We also determined the expression of GPER by flow cytometry after exposing AS-B634 cells for 3 days to each of the ligands. All four agonists significantly increased GPER expression by ~1.4-fold to ~1.9-fold of control cells (1.5-, 1.5-, 1.36- and 1.82-fold for 4-OHT, E2, E3 and G1, respectively; Fig. 4*e*). We next evaluated the effects of the GPER ligands on the stemness of AS-B145 cells. After incubating AS-B145 cells with 4-OHT (2,500 nM), E2 (200 nM), E3 (100 nM) and G1 (100 nM) for 3 days, populations enriched in BCSCs were identified using the ALDEFLOUR assay (Fig. 4*f*). In these experiments, E3 and G1 treatment led to increased $ALDH^+$ cell populations (1.59-fold for E3 and 1.88-fold for G1). Treatment with 4-OHT and E2 led to 1.38-fold and 1.25-fold increases in $ALDH^+$ cell populations, respectively, suggesting that 4-OHT and E2 may not be as effective as E3 and G1 in promoting the stemness of BCSCs. Thus, the activation of GPER indeed promotes stemness.

### Depletion of the GPER inhibits BCSCs tumorigenicity

To determine whether the dysregulated GPER contributes to tumorigenesis *in vivo*, $1 \times 10^5$ of GPER silenced AS-B145 cells (shGPER) and its control cells (shLuc) were implanted into the mammary fat pads of 6- to 8-week-old female NSG mice. Tumor growth was monitored weekly and the mice were sacrificed 2 months after implantation. As shown in Figure 5, knockdown of GPER in AS-B145 cells attenuated the growth of xenograft tumors (Figs. 5*a* and 5*b*). To determine the CSC subpopulation, these tumors were digested into single-cell suspensions and stained with CD24 and CD44 markers, followed by

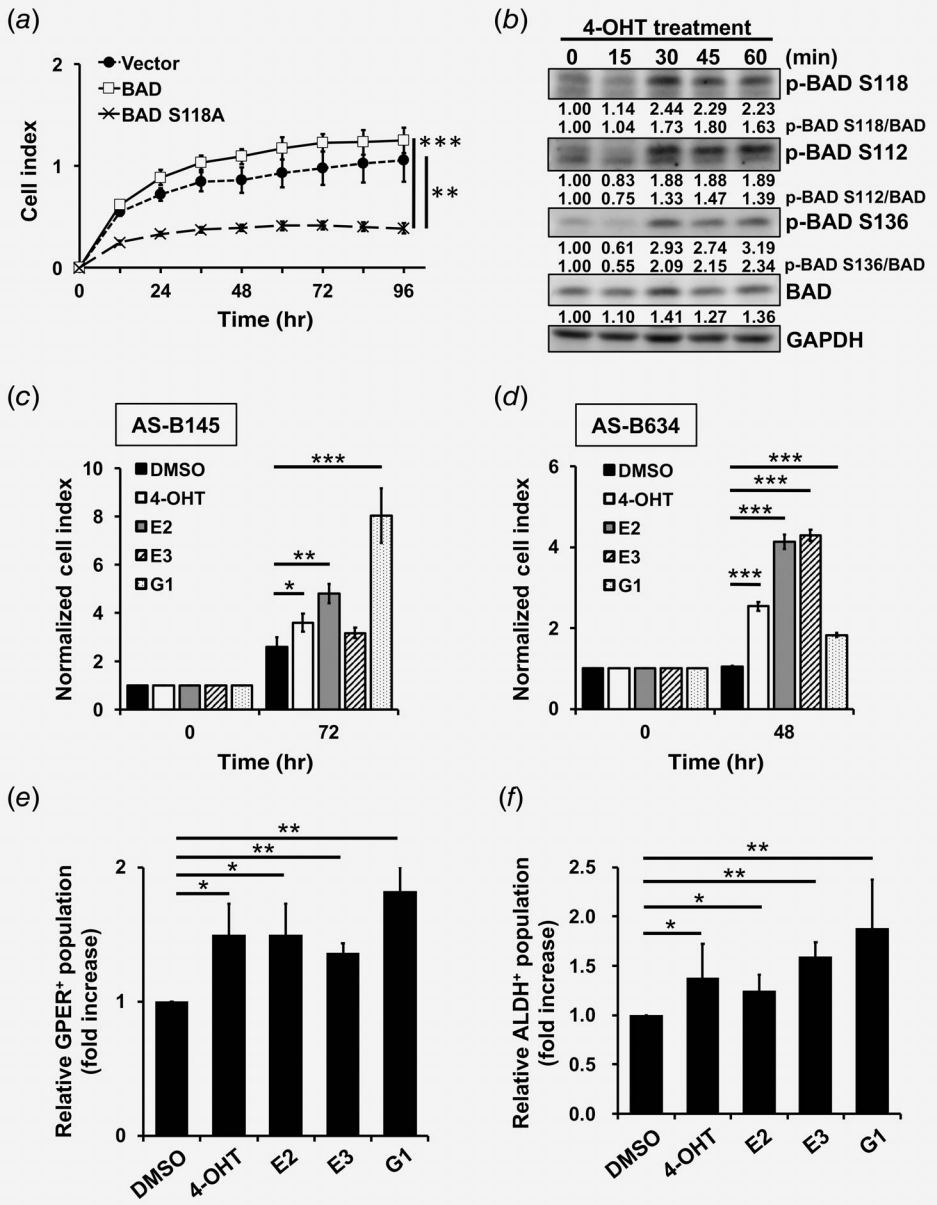


**Figure 4.** GPER signaling included BAD phosphorylation in BCSCs. (*a*) The growth curve of AS-B145 cells expressing the dominant-negative BAD Ser118Ala mutant. AS-B145 cells were infected with a doxycycline-inducible lentiviral vector that expressed the mutant BAD or WT BAD. Cell growth was measured using the xCELLigence system. Values represent mean ± SD, $n = 3$, ***$p < 0.001$ for BAD S118A compared to WT BAD, the cell index at 96 hr was analyzed by one-way ANOVA. (*b*) Total cell lysates prepared from AS-B145 cells that had been treated with 4-OHT (2,500 nM) for 15, 30, 45 or 60 min were immunoblotted. The amount of BAD p-Ser118, p-Ser112 and p-Ser136 was normalized to the corresponding amount of GAPDH, and the fold increase in phosphorylation was normalized to the amount at 0 min. (*c*) AS-B145 cells were treated with 4-OHT (2,500 nM), E2 (200 nM), E3 (100 nM) or G1 (100 nM) for 72 hr. Cell proliferation was assessed using the xCELLigence system. The cell index of treated cells at 0 hr was set as 1.0, and the cell index of treated cells at 72 hr relative to the time zero value. Value represents mean ± SD, $n = 3$, *$p < 0.05$, **$p < 0.01$ and ***$p < 0.001$. The statistic was determined by one-way ANOVA. (*d*) AS-B634 cells were treated with 4-OHT (2000 nM), E2 (50 nM), E3 (100 nM) or G1 (100 nM) for 48 hr. Data presentation as for Figure 4*c*. (*e*) GPER expression of permeabilized AS-B634 cells was assessed by flow cytometry 3 days after treatment with 4-OHT (2000 nM), E2 (50 nM), E3 (100 nM) or G1 (100nM). The GPER$^+$ population of treated cells was presented as fold increase relative to the control group (DMSO). The statistic was determined by one-way ANOVA, $n = 3$, *$p < 0.05$, **$p < 0.01$. (*f*) ALDH activity in AS-B145 cells was assessed by ALDEFLUOR assay after treatment with 4-OHT (2,500 nM), E2 (200 nM), E3 (100 nM) or G1 (100 nM) for 3 days. Cell treated with diethylaminobenzaldehyde (DEAB), which is the inhibitor of ALDH, was used to distinguish ALDH$^+$ from ALDH$^-$ cells. The ALDH$^+$ populations of treated cells were presented as fold increase relative to the control group. The statistic was determined by on way ANOVA, $n = 3$ for 4-OHT, $n = 3$ for E2, $n = 6$ for E3 and $n = 2$ for G1, *$p < 0.05$, **$p < 0.01$.

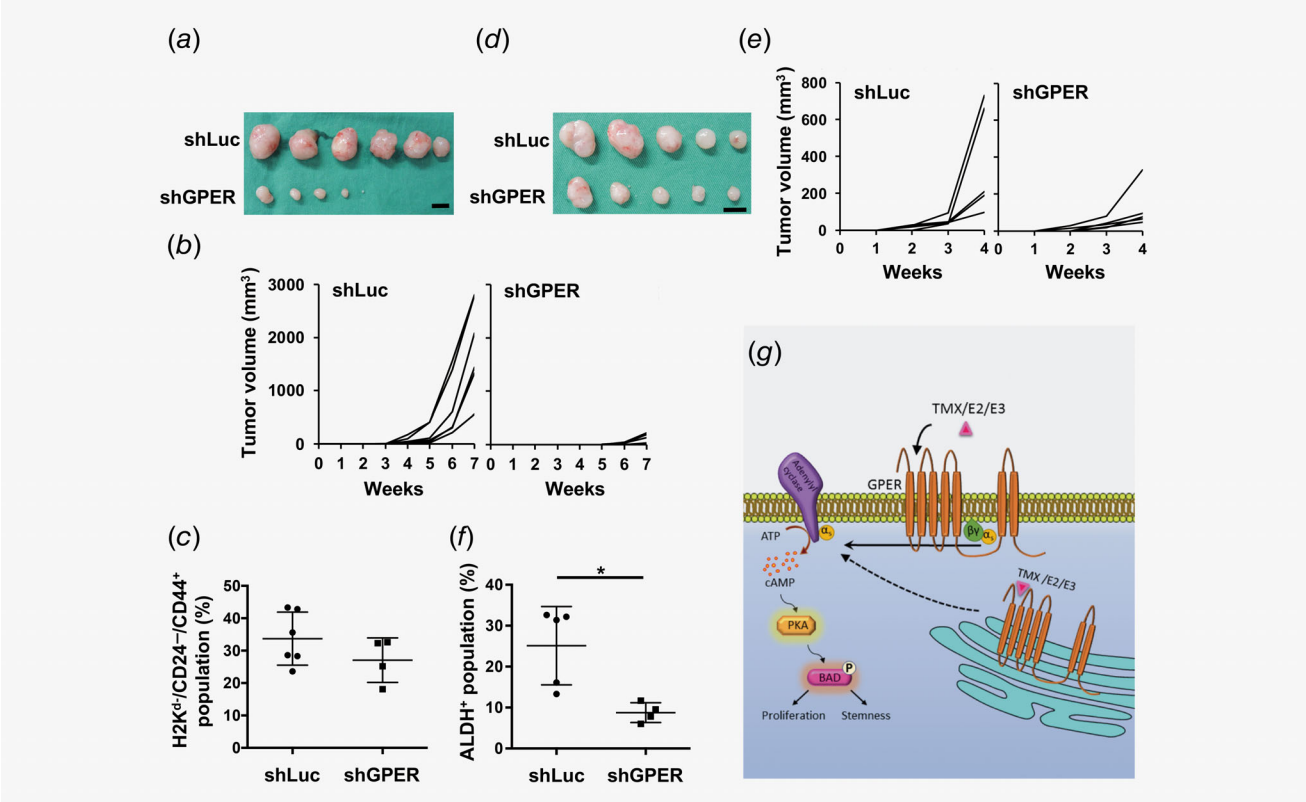


**Figure 5.** The tumorigenicity of GPER in BCSCs. *(a)* AS-B145 cells were infected with lentiviral shLuc or shGPER for 6 days. Cells ($1 \times 10^5$) infected with shRNAs were implanted into the mammary fat pads of 6- to 8-week-old female NSG mice ($n = 6$). Photos show the tumors of individual mice after sacrifice. The black line represents 1 cm. (*b*) The tumor growth curves in individual mice of each group during the 2 months after implantation. (*c*) Due to the small tumor sizes, six shLuc and four shGPER tumors were digested into single cells suspension and stained with $H2K^d$/CD24/CD44 antibodies to determine the BCSC subpopulation. The mean percentages of $H2K^{d-}/CD24^-/CD44^+$ cells in the total tumor cell population in the shLuc and shGPER are shown. Values represent mean ± SD, $p = 0.2$, Student's *t*-test. (*d* and *e*) AS-B634 cells ($5 \times 10^4$) infected with shRNAs were implanted into the mammary fat pads of 6- to 8-week-old NSG mice ($n = 5$). The tumor growth curves in individual mice during the 4 weeks after implantation are shown (five shLuc and five shGPER tumors). (*f*) Tumors (five shLuc and four shGPER tumors) were digested and stained with using the ALDEFLUOR assay. The mean percentages of $ALDH^+$ cells in the total tumor cell population in the shLuc and shGPER groups are shown. Values represent mean ± SD, $^*p < 0.05$, Student's *t*-test. (*g*) Schematic illustration of GPER signal transduction pathway involved in the regulation of survival and stemness of BCSCs. Treatment of $GPER^+$ breast cancer cells with GPER agonists (TMX, E2 and E3) triggers cAMP production, which in turn induces phosphorylation of PKA and BAD, thereby promoting cell proliferation and sustaining CSCs.

flow cytometric analysis. As shown in Figure 5*c*, $CD24^-CD44^+$ cells accounted for 33.7 ± 3.3 and 27.05 ± 3.4% of total cells for shLuc control tumors and shGPER tumors, respectively. The difference between the two percentages was not statistically significant, presumably due to the resurgence of GPER expression in shGPER tumors, which was 1.73-fold the control value in the harvested tumors (Supporting Information Fig. S2). We also examined the tumorigenicity of shRNAs infected AS-B634 cells in NSG mice. As shown in Figures 5*d* and 5*e*, GPER silencing significantly retarded the tumor growth. Furthermore, the CSC subpopulation in the AS-B634 xenograft, as determined by ALDEFLUOR assay, showed that the average percentage of $ALDH^+$ cells was significantly higher in shLuc control tumors than shGPER tumors (25.1 ± 4.3 *vs.* 8.8 ± 1.2), suggesting that GPER may sustain the BCSC properties (Fig. 5*f*). Taken together, these data indicate that GPER and its downstream signaling play a key role in the survival and the stemness of BCSCs.

## Discussion

Previous studies indicated that GPER agonists stimulate GPER-dependent cAMP production in several breast cancer cell lines,[29] and that the estrogen-induced GPER-dependent PKA pathway is critical in ameliorating liver injury.[40] In our study, we provided the first evidence that GPER-initiated signaling *via* PKA activation and BAD Ser118 phosphorylation are crucial for the survival of BCSCs. PKA is known as a cAMP-dependent enzyme consisting of regulatory and catalytic subunits. PRKAR1A, one of four PKA regulatory subunits, is important for the specific activities of PKA catalytic subunits and for the subcellular localization of PKA. Increased PRKAR1A expression in human breast carcinomas has been shown to correlate with active malignant cell growth and poor prognosis.[41] Reduction of PRKAR1A expression by antisense inhibition causes growth inhibition and apoptosis, which is attributed to hypophosphorylation of BAD and hyperphosphorylation of Bcl-2.[42] In our phosphoproteomics

studies, not only was Thr197 of PRKACA highly phosphorylated in BCSCs but the phosphorylation at Ser83 of PRKAR1A was higher in BCSCs than non-BCSCs (Supporting Information Table S1). However, the exact role of phosphorylation at Ser83 of PRKAR1A in the regulation of the PKA holoenzyme and in BCSCs remains unclear and awaits future studies. Moreover, phosphorylation of BAD Ser118 results in increased glucokinase activation with ensuing ATP production in mitochondria,[43] which could account for our observed increases in proliferation of breast cancer and BCSCs upon exposure to GPER agonists. Increased phosphorylation of PRKAR1A Ser83 and BAD Ser118 may, therefore, contribute to BCSC survival.

There is increasing evidence for the importance of modulating GPER signaling in the treatment of breast cancer. In recent years, many chemicals have been identified as agonists or antagonists of GPER.[44] Although 4-OHT, E2, E3 and G1 have been reported to be GPER ligands, their downstream signals exhibited both overlapping and unique profiles, even within the same breast cancer cell line.[45] In our studies, this is further complicated since two different PDXs and their derived cell lines which may contribute to variations in their responses to each chemical. Among the four GPER agonists investigated, G1 appeared to induce greater increases in the number of $GPER^+$ cells and $ALDH^+$ cells than the others. This might reflect greater specificity of G1 for GPER than the others. Furthermore, pathologic features such as ER, PR and HER2 status may also affect GPER signaling. Although GPER expression had no correlation with the status of ER, PR and HER2 expression in primary breast cancers,[46] the crosstalk between GPER and ErbB receptors has been reported. For instance, EGFR transactivation upon activation of GPER has been documented in breast cancer.[7] In addition, since certain ER antagonist, such as TMX may serve as GPER agonist,[11] the expression status of ER may affect the response of GPER expressing cells to TMX. In view of the complex interactions between GPER and ER/PR/HER2 pathways, ER-negative PDXs used in our study may lessen the impact of ER on GPER signaling. Our findings not only demonstrated a key role of GPER in the survival and tumor-initiation capacity of BCSCs but also provide a molecular mechanism underlying increased tumorigenicity mediated by GPER.

Current evidence suggests that subpopulations of cancer cells with stem cell-like properties may drive tumor growth and metastasis.[15] By virtue of their relative resistance to current therapeutic approaches, these cells may contribute to treatment failure and relapse. Thus, to improve therapeutic efficacy, other strategies must be developed to effectively target populations of cancer stem cells. However, the signal transduction pathways important to stem cell properties have not been systematically elucidated. In our phosphoproteomics analyses, we identified 455 phosphoproteins that were differentially regulated in many of the signal transduction pathways associated with the stemness characteristics of self-renewal and cell survival, as well as with tumorigenesis. These signal pathways and their networking revealed many phosphoproteins with unknown functions as well as novel phosphorylation sites of known proteins, which may be targeted for future investigations.

GPER plays a multifaceted role in metabolic disorder[47] and cancer. In cancer progression, GPER can encourage the growth of breast cancer cells *via* the upregulation of c-Fos.[48] Besides, GPER enhances cellular adhesivity and fibronectin matrix assembly and allows for anchorage-independent growth *via* Shc-dependent pathway.[49] In addition, GPER can promote the process of epithelial–mesenchymal transition (EMT) *via* upregulating Snail expression through the crosstalk between GPER and the Notch signaling pathway, as demonstrated by incubating breast cancer cell line with estradiol.[50] Another study has demonstrated that GPER agonists-induced signaling in cancer-associated fibroblasts upregulates the expression of connective tissue growth factor (*CTGF*), which in turn promotes migration of breast cancer cells.[8] Apart from these possible mechanisms by which GPER may contributes to carcinogenesis, we found that GPER agonists increased cell proliferation and the BCSC population *via* p-PKA/p-BAD signaling (Fig. 5*g*). In conclusion, our studies revealed a vital role of GPER-mediated signaling pathways in BCSC survival, suggesting that the identification of GPER-specific antagonists may provide new therapies for breast cancer.

## Acknowledgements

We are grateful to the National RNAi Core Facility, Academia Sinica, Taipei, Taiwan, for providing lentiviral plasmids. We thank Hsiao-Wei Wu for her excellent scientific illustration. This work was supported by the grants from the Ministry of Science and Technology in Taiwan (NSC102-2321-B-182A-005, MOST 103-2321-B-182A-002, MOST 104-2321-B-182A-004), Academia Sinica (97-2628-M-001-020-MY3), Chang Gung Medical Foundation (OMRPG3C0012, OMRPG3C0013) and Chang Gung Postdoctoral Fellowship Award.

## References

1. Chen JQ, Russo J. ERα-negative and triple negative breast cancer: molecular features and potential therapeutic approaches. *Biochim Biophys Acta* 2009;1796:162–75.
2. Lonard DM, Smith CL. Molecular perspectives on selective estrogen receptor modulators (SERMs): progress in understanding their tissue-specific agonist and antagonist actions. *Steroids* 2002;67:15–24.
3. Shao W, Brown M. Advances in estrogen receptor biology: prospects for improvements in targeted breast cancer therapy. *Breast Cancer Res* 2004;6:39–52.
4. Jameera Begam A, Jubie S, Nanjan MJ. Estrogen receptor agonists/antagonists in breast cancer therapy: a critical review. *Bioorg Chem* 2017;71:257–74.
5. Osborne CK, Schiff R. Mechanisms of endocrine resistance in breast cancer. *Annu Rev Med* 2011;62:233–47.
6. Carmeci C, Thompson DA, Ring HZ, et al. Identification of a gene (GPR30) with homology to the G-protein-coupled receptor superfamily associated with estrogen receptor expression in breast cancer. *Genomics* 1997;45:607–17.

7. Filardo EJ. Epidermal growth factor receptor (EGFR) transactivation by estrogen via the G-protein-coupled receptor, GPR30: a novel signaling pathway with potential significance for breast cancer. *J Steroid Biochem Mol Biol* 2002;80:231–8.
8. Pandey DP, Lappano R, Albanito L, et al. Estrogenic GPR30 signalling induces proliferation and migration of breast cancer cells through CTGF. *EMBO J* 2009;28:523–32.
9. Marjon NA, Hu C, Hathaway HJ, et al. G protein-coupled estrogen receptor regulates mammary tumorigenesis and metastasis. *Mol Cancer Res* 2014;12:1644–54.
10. Vivacqua A, Bonofiglio D, Albanito L, et al. 17beta-estradiol, genistein, and 4-hydroxytamoxifen induce the proliferation of thyroid cancer cells through the g protein-coupled receptor GPR30. *Mol Pharmacol* 2006;70:1414–23.
11. Ignatov A, Ignatov T, Roessner A, et al. Role of GPR30 in the mechanisms of tamoxifen resistance in breast cancer MCF-7 cells. *Breast Cancer Res Treat* 2010;123:87–96.
12. Catalano S, Giordano C, Panza S, et al. Tamoxifen through GPER upregulates aromatase expression: a novel mechanism sustaining tamoxifen-resistant breast cancer cell growth. *Breast Cancer Res Treat* 2014;146:273–85.
13. Ignatov A, Ignatov T, Weissenborn C, et al. G-protein-coupled estrogen receptor GPR30 and tamoxifen resistance in breast cancer. *Breast Cancer Res Treat* 2011;128:457–66.
14. Weissenborn C, Ignatov T, Ochel HJ, et al. GPER functions as a tumor suppressor in triple-negative breast cancer cells. *J Cancer Res Clin Oncol* 2014;140:713–23.
15. Visvader JE, Lindeman GJ. Cancer stem cells in solid tumours: accumulating evidence and unresolved questions. *Nat Rev Cancer* 2008;8:755–68.
16. Lorico A, Rappa G. Phenotypic heterogeneity of breast cancer stem cells. *J Oncol* 2011;2011:135039.
17. Phillips TM, McBride WH, Pajonk F. The response of CD24(−/low)/CD44+ breast cancer-initiating cells to radiation. *J Natl Cancer Inst* 2006;98:1777–85.
18. Liu S, Wicha MS. Targeting breast cancer stem cells. *J Clin Oncol* 2010;28:4006–12.
19. Croker AK, Allan AL. Inhibition of aldehyde dehydrogenase (ALDH) activity reduces chemotherapy and radiation resistance of stem-like $ALDH^{hi}CD44^{+}$ human breast cancer cells. *Breast Cancer Res Treat* 2012;133:75–87.
20. Zhou J, Wulfkuhle J, Zhang H, et al. Activation of the PTEN/mTOR/STAT3 pathway in breast cancer stem-like cells is required for viability and maintenance. *Proc Natl Acad Sci USA* 2007;104:16158–63.
21. Chang WW, Lin RJ, Yu J, et al. The expression and significance of insulin-like growth factor-1 receptor and its pathway on breast cancer stem/-progenitors. *Breast Cancer Res* 2013;15:R39.
22. Chang WW, Lee CH, Lee P, et al. Expression of Globo H and SSEA3 in breast cancer stem cells and the involvement of fucosyl transferases 1 and 2 in Globo H synthesis. *Proc Natl Acad Sci USA* 2008;105:11667–72.
23. Fu CH, Lin RJ, Yu J, et al. A novel oncogenic role of inositol phosphatase SHIP2 in ER-negative breast cancer stem cells: involvement of JNK/-vimentin activation. *Stem Cells* 2014;32:2048–60.
24. Tsai CF, Wang YT, Chen YR, et al. Immobilized metal affinity chromatography revisited: pH/acid control toward high selectivity in phosphoproteomics. *J Proteome Res* 2008;7:4058–69.
25. Wang YT, Tsai CF, Hong TC, et al. An informatics-assisted label-free quantitation strategy that depicts phosphoproteomic profiles in lung cancer cell invasion. *J Proteome Res* 2010;9:5582–97.
26. Tsou CC, Tsai CF, Tsui YH, et al. IDEAL-Q, an automated tool for label-free quantitation analysis using an efficient peptide alignment approach and spectral data validation. *Mol Cell Proteomics* 2010;9:131–44.
27. Zeeberg BR, Feng W, Wang G, et al. GoMiner: a resource for biological interpretation of genomic and proteomic data. *Genome Biol* 2003;4:R28.
28. Ekins S, Nikolsky Y, Bugrim A, et al. Pathway mapping tools for analysis of high content data. *Methods Mol Biol* 2007;356:319–50.
29. Sandén C, Broselid S, Cornmark L, et al. G protein-coupled estrogen receptor 1/G protein-coupled receptor 30 localizes in the plasma membrane and traffics intracellularly on cytokeratin intermediate filaments. *Mol Pharmacol* 2011;79:400–10.
30. Cheng SB, Quinn JA, Graeber CT, et al. Down-modulation of the G-protein-coupled estrogen receptor, GPER, from the cell surface occurs via a trans-Golgi-proteasome pathway. *J Biol Chem* 2011;286:22441–55.
31. Yu B, Sun X, Shen HY, et al. Expression of the apoptosis-related genes BCL-2 and BAD in human breast carcinoma and their associated relationship with chemosensitivity. *J Exp Clin Cancer Res* 2010;29:107.
32. Garcia-Castillo J, Pedersen K, Angelini PD, et al. HER2 carboxyl-terminal fragments regulate cell migration and cortactin phosphorylation. *J Biol Chem* 2009;284:25302–13.
33. Peck D, Isacke CM. Hyaluronan-dependent cell migration can be blocked by a CD44 cytoplasmic domain peptide containing a phosphoserine at position 325. *J Cell Sci* 1998;111(Pt 11):1595–601.
34. Lian I, Kim J, Okazawa H, et al. The role of YAP transcription coactivator in regulating stem cell self-renewal and differentiation. *Genes Dev* 2010;24:1106–18.
35. Decker T, Kovarik P. Serine phosphorylation of STATs. *Oncogene* 2000;19:2628–37.
36. Prossnitz ER, Arterburn JB, Smith HO, et al. Estrogen signaling through the transmembrane G protein-coupled receptor GPR30. *Annu Rev Physiol* 2008;70:165–90.
37. Taylor SS, Kim C, Cheng CY, et al. Signaling through cAMP and cAMP-dependent protein kinase: diverse strategies for drug design. *Biochim Biophys Acta* 2008;1784:16–26.
38. Sastry KS, Al-Muftah MA, Li P, et al. Targeting proapoptotic protein BAD inhibits survival and self-renewal of cancer stem cells. *Cell Death Differ* 2014;21:1936–49.
39. Tan Y, Demeter MR, Ruan H, et al. BAD Ser-155 phosphorylation regulates BAD/Bcl-XL interaction and cell survival. *J Biol Chem* 2000;275:25865–9.
40. Hsieh YC, Yu HP, Frink M, et al. G protein-coupled receptor 30-dependent protein kinase a pathway is critical in nongenomic effects of estrogen in attenuating liver injury after trauma-hemorrhage. *Am J Pathol* 2007;170:1210–8.
41. Wilkes D, Charitakis K, Basson CT. Inherited disposition to cardiac myxoma development. *Nat Rev Cancer* 2006;6:157–65.
42. Cho YS, Kim MK, Tan L, et al. Protein kinase a RIα antisense inhibition of PC3M prostate cancer cell growth: *Bcl*-2 hyperphosphorylation, Bax up-regulation, and bad-Hypophosphorylation. *Clin Cancer Res* 2002;8:607–14.
43. Danial NN. BAD: undertaker by night, candyman by day. *Oncogene* 2008;27(Suppl 1):S53–70.
44. Lappano R, Maggiolini M. G protein-coupled receptors: novel targets for drug discovery in cancer. *Nat Rev Drug Discov* 2011;10:47–60.
45. Smith LC, Ralston-Hooper KJ, Ferguson PL, et al. The G protein-coupled estrogen receptor agonist G-1 inhibits nuclear estrogen receptor activity and stimulates novel Phosphoproteomic signatures. *Toxicol Sci* 2016;151:434–46.
46. Luo HJ, Luo P, Yang GL, et al. G-protein coupled estrogen receptor 1 expression in primary breast cancers and its correlation with Clinicopathological variables. *J Breast Cancer* 2011;14:185–90.
47. Shi H, Kumar SP, Liu X. G protein-coupled estrogen receptor in energy homeostasis and obesity pathogenesis. *Prog Mol Biol Transl Sci* 2013;114:193–250.
48. Maggiolini M, Vivacqua A, Fasanella G, et al. The G protein-coupled receptor GPR30 mediates c-fos up-regulation by 17beta-estradiol and phytoestrogens in breast cancer cells. *J Biol Chem* 2004;279:27008–16.
49. Magruder HT, Quinn JA, Schwartzbauer JE, et al. The G protein-coupled estrogen receptor-1, GPER-1, promotes fibrillogenesis via a Shc-dependent pathway resulting in anchorage-independent growth. *Horm Cancer* 2014;5:390–404.
50. Pupo M, Pisano A, Abonante S, et al. GPER activates notch signaling in breast cancer cells and cancer-associated fibroblasts (CAFs). *Int J Biochem Cell Biol* 2014;46:56–67.